iScience

CellPress
OPEN ACCESS

Article

Optimum Threshold Minimizes Noise in Timing of Intracellular Events

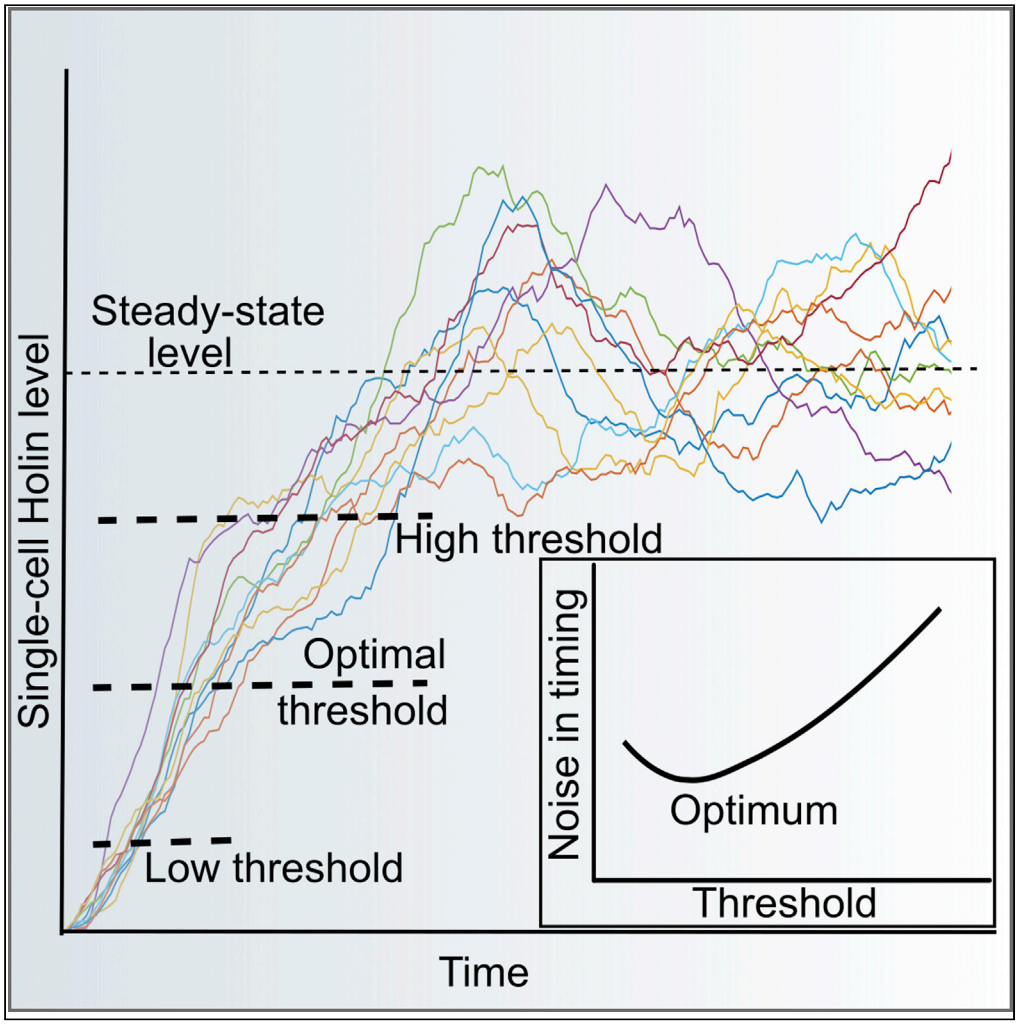

Sherin Kannoly, Tianhui Gao, Supravat Dey, Ing-Nang Wang, Abhyudai Singh, John J. Dennehy

absingh@udel.edu (A.S.)
john.dennehy@qc.cuny.edu (J.J.D.)

HIGHLIGHTS

Mutations in timekeeper protein alter event timing and noise in event timing

Data show noise in event timings follow a concave up shape with increasing threshold

Mathematical modeling identifies optimal threshold minimizing noise in event timing

Results imply that noise in event timing can be a target of natural selection

Kannoly et al., iScience *23*, 101186
June 26, 2020
https://doi.org/10.1016/j.isci.2020.101186

iScience

CellPress
OPEN ACCESS

Article

Optimum Threshold Minimizes Noise in Timing of Intracellular Events

Sherin Kannoly,[1] Tianhui Gao,[1] Supravat Dey,[3] Ing-Nang Wang,[2] Abhyudai Singh,[3,*] and John J. Dennehy[1,4,5,*]

SUMMARY

How the noisy expression of regulatory proteins affects timing of intracellular events is an intriguing fundamental problem that influences diverse cellular processes. Here we use the bacteriophage λ to study event timing in individual cells where cell lysis is the result of expression and accumulation of a single protein (holin) in the *Escherichia coli* cell membrane up to a critical threshold level. Site-directed mutagenesis of the holin gene generated phage variants that vary in their lysis times from 30 to 190 min. Observation of the lysis times of single cells reveals an intriguing finding—the noise in lysis timing first decreases with increasing lysis time to reach a minimum and then sharply increases at longer lysis times. A mathematical model with stochastic expression of holin together with dilution from cell growth was sufficient to explain the non-monotonic noise profile and identify holin accumulation thresholds that generate precision in lysis timing.

INTRODUCTION

The inherent probabilistic nature of biochemical reactions and low copy numbers of molecules involved result in significant random fluctuations (noise) in protein levels inside isogenic cells inhabiting the same environment (Bar-Even et al., 2006; Cai et al., 2006; Eldar and Elowitz, 2010; Elowitz et al., 2002; Raj and van Oudenaarden, 2008; Taniguchi et al., 2010). Although the origins of stochastic gene expression have been extensively studied across organisms, the impacts of the noisy expression of key regulatory proteins on the timing of intracellular events is underappreciated (Liu et al., 2017; Song et al., 2015; Song and Acar, 2019; Yurkovsky and Nachman, 2013). Identifying regulatory motifs that buffer randomness in the timing of intracellular events has important consequences for disparate cellular processes, such as apoptosis, cell-cycle control, cell differentiation, and sporulation, where precision required for proper system functioning depends on regulatory molecules reaching critical threshold levels at the right time. For instance, cell heterogeneity in concentrations of holin homologues, Bax/Bak (Pang et al., 2011), may determine a cell's propensity for apoptosis (Santos et al., 2019). Mutations promoting apoptosis resistance may give rise to cells with higher tumorigenic potential (i.e., cancer stem-like cells) (Campbell and Tait, 2018). In another example, proper timing of yeast cell division is ensured by the precise expression of a regulatory protein, Cln, up to a critical threshold level (Schneider et al., 2004). Despite these significant impacts, how cells maintain precision in event timing despite noisy gene expression remains poorly understood.

To address this knowledge gap, we employ the bacteriophage λ as a model system for studying event timing at the single cell level. Here, an easily observable event (cell lysis) is the result of the expression and accumulation of a single regulatory protein (holin) in the *Escherichia coli* cell inner membrane up to a threshold level (Figure 1A) (Wang et al., 2000; Young, 2014). Once holin surpasses this critical threshold concentration, it nucleates to form large holes in the inner membrane, triggering events that result in the destruction of the cell and the release of phage progeny (Wang et al., 2000; Young, 2014). Since holin nucleation and cell lysis are essentially simultaneous, holin can be said to be the timekeeper of the lysis event (White et al., 2011).

Single-cell observations of holin-induced lysis allows the calculation of both the mean and noise of lysis timing, where noise is quantified using a dimensionless metric, the coefficient of variation (standard deviation divided by the mean). Our prior work revealed incredible precision in lysis timing in the wild-type λ strain: lysis occurs on average at 65 min with a coefficient of variation of less than 5% (Dennehy and Wang, 2011; Singh and Dennehy, 2014).

[1]Biology Department, Queens College of The City University of New York, Queens, NY, USA

[2]Department of Biological Sciences, University at Albany, Albany, NY, USA

[3]Department of Electrical and Computer Engineering, University of Delaware, Newark, DE, USA

[4]The Graduate Center of The City University of New York, New York City, NY, USA

[5]Lead Contact

*Correspondence: absingh@udel.edu (A.S.), john.dennehy@qc.cuny.edu (J.J.D.)

https://doi.org/10.1016/j.isci.2020.101186

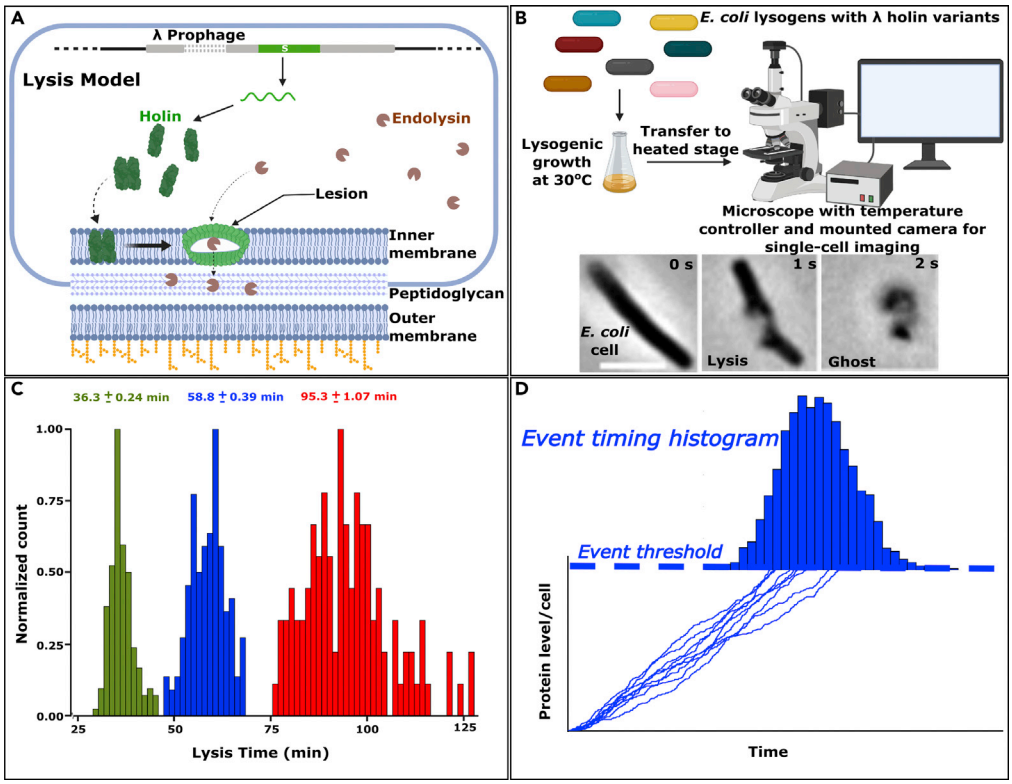

Figure 1. Phage Lambda Model System Can Be Manipulated to Study Lysis Time Variation

(A) Lysis model showing cell lysis mediated by λ holin. Accumulation of holin in the inner cell membrane results in lesions, which trigger cell lysis by allowing endolysin to access the *E. coli* cell wall.

(B) Lysogens were used for single-cell imaging and recording of lysis events. Inset panels track the lysis event occurring in a single cell after induction (original images courtesy of Ry Young; scale bar, 5 μm). The third image shows the cell debris (ghost) after lysis.

(C) Lysis time distributions for three lysogens (~100 cells) with different means (green, M1L/I87L; blue, S105; red, M1L/G39S). Mean ± SEM values are shown for each distribution.

(D) Cartoon showing stochastic accumulation of holin over time, and lysis time is the first-passage time (FPT) for holin levels to reach a critical threshold. Since expression is stochastic, the threshold is reached at different times in different cells.

Despite this precision, different holin mutants exhibited a wide range of means and noise in lysis time (Dennehy and Wang, 2011). The sources of this noise may include variations in the rate of transcription of λ late mRNA, the rate of holin protein translation by host ribosomes, the rate of holin insertion into the plasma membrane, and the holin concentration required for triggering membrane hole formation. In our formulations, the latter two factors were combined into a single parameter, threshold concentration.

To explore how variations in these parameters affect lysis time noise, we mathematically modeled lysis time as the first-passage time for membrane holin levels to cross a critical threshold (Singh and Dennehy, 2014). We employed stochastic gene expression models to derive the exact analytical formulae for the first-passage time moments (Singh and Dennehy, 2014). These formulae were used to generate predictions of how changes in holin transcription and translation efficiencies and holin threshold concentrations can modulate the lysis time mean and variation (Singh and Dennehy, 2014).

The key objective of the work described here is to investigate experimentally how manipulation of the lysis threshold affects the noise in lysis timing. To this end, we systematically altered the amino acid sequence of the holin protein in order to shift (both increase or decrease) the lysis threshold (Ghusinga et al., 2017; Singh and Dennehy, 2014). These amino acid sequence changes may affect holin structure, dimerization and/or oligomerization potential, and/or membrane insertion capacity. Sequence alterations that inhibit holin's ability to pass into the inner membrane may, for example, increase the threshold, whereas alterations

increasing holin-holin affinity may decrease the threshold. This contribution studies the effects of these alterations on noise in lysis timing both experimentally and via mechanistic mathematical models to uncover an intriguing insight—precision in timing is enhanced at an intermediate threshold.

RESULTS AND DISCUSSION

Timing of intracellular events is often studied using a first-passage time (FPT) framework that captures the first time a random process crosses a threshold (Co et al., 2017; Ghusinga et al., 2016; Gupta et al., 2018). In our prior work, we formulated lysis timing as an FPT problem (Ghusinga et al., 2017; Singh and Dennehy, 2014). Here, the onset of transcription from λ's late promoter results in stochastic accumulation of holin within the host cell membrane, and cell lysis is triggered when the total cellular holin concentration reaches a critical threshold (Figure 1D). Our mathematical analysis predicted that noise in timing is inversely proportional to the threshold (Ghusinga et al., 2017; Singh and Dennehy, 2014). The logical progression of this work is to verify this prediction through experimental manipulation of the lysis threshold by altering the holin sequence, which has the effect of altering lysis time mean and noise (Dennehy and Wang, 2011).

It is important to point out that the holin gene *S* of wild-type λ has two translation initiation sites. Gene expression results in the production of two proteins, holin and antiholin, in a 2:1 ratio ensuring excess holin (Chang et al., 1995). Antiholin has two extra residues, a methionine and a leucine, and acts antagonistically to holin, which has the lysis function (Bläsi et al., 1990; Gründling et al., 2000). For the sake of simplicity, we have not considered the effects of antiholin in our model. Although antiholin binding inhibits holin function and thereby delays lysis by several minutes, the biological relevance of this inhibition is still unclear. A simplistic view is that antiholin expression is favored when a delay in lysis is beneficial under adverse growth conditions. However, this has not been conclusively demonstrated so far. Moreover, any mutations in holin would also be incorporated in antiholin as they are encoded from the same gene with different start sites. Thus, to remove any confounding effects of antiholin on lysis timing, we introduced mutations into a strain of λ where antiholin expression has been abolished via the M1L mutation (Table 1).

Site-directed mutagenesis was used to introduce one or two nucleotide substitutions into plasmids bearing the *S105* holin allele. The resulting plasmids were used to generate a library of *E. coli* lysogens differing from the *S105* mutant by one or two amino acid substitutions in the holin gene. The optical densities of thermally induced batch cultures of these lysogens were tracked to determine their lysis times (unpublished data). For this study, we selected a subset of twenty holin mutants spanning a wide range of mean lysis times (Table 1). For each mutant strain, we thermally induced and recorded single cell lysis events for ~100 cells using a microscope-mounted, temperature-controlled perfusion chamber (Figures 1B and 1C, Video S1). This set up resembles a continuous culture system where fresh media is pumped over immobilized cells and waste removed at a constant rate. This allows normal cell growth and metabolism observed as increase in cell length, which facilitates phage multiplication culminating in lysis. The mean lysis times calculated using both the batch culture and single-cell recordings were strongly correlated (Figure S1).

Using a subset of lysogens, we verified that the holin mutations had no effect on holin expression via western blot assays of holin levels in whole-cell extracts (Figure S2). Therefore, any effects on lysis timing can be attributed to shifting of lysis threshold as a result of the amino acid changes in the holin gene. These mutations in holin may affect lysis timing by altering holin-holin affinity, holin accession to the inner membrane, and/or holin nucleation within the inner membrane. To investigate these possibilities further, we compared levels of different holin mutants in the cell membrane. Interestingly, a mutant with short lysis time showed almost 5-fold higher holin levels in the membrane compared with the wild-type (Figure S2). Contrarily, a mutant with long lysis time showed holin levels comparable with the wild-type. In the latter case, the mutated holin might be impaired in the formation of membrane lesions required for lysis, and thus delay lysis. These results suggest that the quality of holin may directly affect the quantity of holin in the membrane and/or its ability to form the membrane lesions critical for lysis. Further biochemical studies may reveal how structural changes in holin affect the different steps leading to cell lysis.

Next, we quantified single-cell FPTs by subtracting 15 min from the recorded lysis times. This 15-min duration accounts for the time delay between lysogen induction and start of transcription from λ's late promoter (Kobiler et al., 2005; Liu et al., 2013). Recall that simple models predict the noise in FPT to monotonically decrease with increasing lysis threshold (and hence, increasing mean FPT) (Singh and Dennehy, 2014).

Strain	Holin Mutations[a]	n[b]	Mean FPT (min) (95% Confidence Interval)[c]	FPT CV^2 (95% Confidence Interval)[c]
JJD3 (WT)	None	120	48.83 (48.14–49.54)	0.007 (0.0051–0.0089)
JJD5 (S105)	M1L	140	43.77 (43.02–44.53)	0.011 (0.0089–0.0137)
JJD246	M1L/H7D	114	54.02 (52.86–55.16)	0.013 (0.0097–0.0179)
JJD248	M1L/F94C	121	41.01 (40.23–41.8)	0.012 (0.0094–0.0157)
JJD251	M1L/A99V	128	25.89 (25.24–26.52)	0.02 (0.0158–0.0237)
JJD253	M1L/L10M	149	26.19 (25.51–26.86)	0.026 (0.0183–0.0337)
JJD388	M1L/L25V/N37H	99	175.09 (163.8–186.1)	0.10 (0.0627–0.1492)
JJD390	M1L/A11G/Y31H	143	170.65 (159.9–181.3)	0.13 (0.1116–0.1581)
JJD391	M1L/A16G/K92Q	115	125.94 (122–130.1)	0.031 (0.0156–0.0488)
JJD404	M1L/I21V	116	15.18 (14.63–15.74)	0.038 (0.0253–0.052)
JJD405	M1L/V45G	118	17.13 (16.7–17.56)	0.02 (0.0147–0.0259)
JJD411	M1L/D85G	91	161.76 (152.4–171.4)	0.086 (0.0699–0.1042)
JJD413	M1L/I87L	158	21.32 (20.86–21.78)	0.020 (0.0157–0.025)
JJD414	M1L/L90I	174	29.96 (29.2–30.7)	0.029 (0.0229–0.0348)
JJD415	M1L/I91T	166	29.11 (28.37–29.85)	0.03 (0.0241–0.0358)
JJD426	M1L/G38S	100	140.26 (134–146.5)	0.053 (0.0374–0.0695)
JJD428	M1L/G39S	111	80.31 (78.23–82.38)	0.02 (0.015–0.0252)
JJD432	M1L/S89W	132	92.74 (90.95–94.61)	0.013 (0.0093–0.0176)
JJD434	M1L/D8G	104	76.09 (74.3–77.93)	0.015 (0.01–0.025)
JJD436	M1L/K92N	138	85.99 (83.86–88.12)	0.021 (0.0116–0.03)

Table 1. Mean and Noise in First-Passage Time (FPT) of Isogenic *E. coli* λ Lysogens

Single-cell FPTs were calculated by subtracting 15 min from the recorded lysis times to account for the time delay between induction and start of transcription from the λ's late promoter.

WT, wild-type.

[a]Amino acid substitutions.

[b]Number of cells observed.

[c]95% CIs after bootstrapping (1,000 replicates).

Computations of both the mean and noise in FPTs across holin mutants as illustrated in Table 1 reveals an intriguing result—for short-lysis strains decreasing the lysis threshold increases the noise consistent with our previous model. By contrast, the data for long-lysis strains *contradicts* our simple model; increasing the lysis threshold *increases* the FPT noise level (Figure 2). The concave-up shape of the plot implies that noise in FPT is minimized at an intermediate threshold. Interestingly, the wild-type λ genotype resides near the base of this plot suggesting that buffering noise in lysis timing is ecologically relevant and is consistent with the existence of optima in lysis timing (Dennehy and Wang, 2011; Heineman et al., 2007; Wang, 2006; Wang et al., 1996).

To explain this non-monotonic noise profile, we developed an expanded model for noisy holin expression (see section S3). Given that the expressed holin proteins are long-lived and do not degrade over relevant timescales (Gründling et al., 2000; White et al., 2010), their turnover is primarily governed by dilution from cellular growth. As has been shown for *E. coli* genes (Cai et al., 2006; Chong et al., 2014; Friedman et al., 2006), we consider holin expression occurring in stochastic bursts with holin dilution occurring between two successive burst events. Subsequent analysis of the model predicts the mean FPT as (details in Supplemental Information)

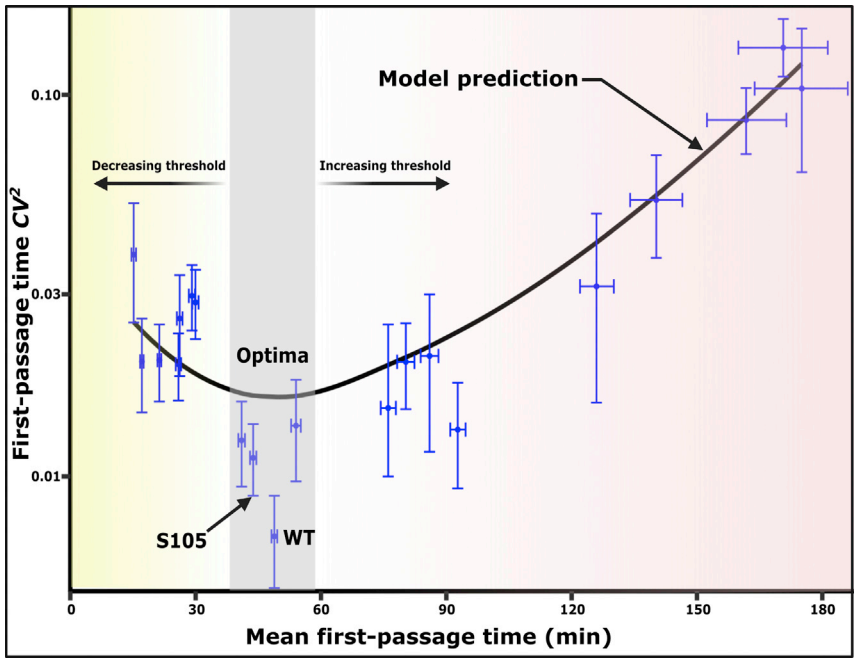

Figure 2. Noise in Lysis Timing Is Minimized at Intermediate Threshold

Noise in first-passage time (FPT) as quantified using the coefficient of variation squared (CV^2) is shown plotted against mean FPT across holin mutants. Each point represents an isogenic λ strain with amino acid substitutions (Table 1) affecting the lysis threshold. These mutants show changes in FPT and CV^2 consistent with the model prediction (black line, Equation 2). Equation 2 was fitting to the data considering a 40-min cell doubling time (i.e., *E. coli* growth at 30°C), with a single-fitting parameter CV_x, which was estimated to be $CV_x = 0.05$. Threshold is optimal at the base of the plot where the noise is minimized. WT, λ strain with wild-type *S* gene; S105, λ strain bearing the *S105* allele (holin); error bars, 95% CIs after bootstrapping (1,000 replicates).

$$\langle FPT \rangle = -\frac{1}{\gamma}\log\left(1-\frac{X}{x_s}\right), \qquad \text{(Equation 1)}$$

where γ is the cellular growth rate, X is the lysis threshold, and x_s is the steady-state mean holin concentration reached after a long time if there was no lysis. Moreover, the noise in FPT was derived as

$$CV^2_{FPT} = CV^2_x \frac{\left[e^{2\gamma\langle FPT\rangle}-1\right]}{(\gamma\langle FPT\rangle)^2}, \qquad \text{(Equation 2)}$$

where CV^2_x quantifies the extent of stochasticity in holin expression. It is important to point out that CV^2_x is determined by the frequency and size of expression bursts (see Equation S13), which in turn depend on transcription and translation rates, respectively. As holin expression levels are unaltered across mutants, we consider CV^2_x to be a constant as the mean FPT is varied with increasing lysis threshold. Intriguingly, this formula predicts the timing noise to vary non-monotonically with the mean FPT and provides an excellent fit to the data (black line in Figure 2). A key insight from (2) is that the noise is minimal when the threshold is 55% of the steady-state holin concentration x_s. Intuitively, when the threshold is low, lysis results from a few bursting events, and increasing the threshold suppresses noise through more effective time averaging of burst events. In contrast, at a high threshold close to the steady-state holin level, the holin concentration starts saturating and crossing the threshold becomes a noise-driven event. In this regime, increasing the threshold enhances noise as holin concentration trajectories become even more shallower. In summary, our study uncovers mechanisms for generating precision in the timing of cellular events given the unavoidable constraints of stochastic gene expression and dilution from cellular growth. We first show that genetic variation in event-timing noise exists. We additionally show that this noise follows a consistent pattern where mutations increasing or decreasing the event threshold relative to an optimum value increases noise.

These results suggest that event timing noise may be a feature of cellular event timing systems that is amenable to natural selection. For critical cellular processes, such as apoptosis, cell division, and cell

differentiation, the structure and functionality of regulatory molecules may be optimized to buffer randomness in event timing. If true, noise minimization may factor in trade-offs associated with the evolution of regulatory molecules involved in cellular event timing.

Our results imply that the structure and activity of phage λ's holin molecule itself is not only evolved to trigger host lysis at an appropriate time (Wang, 2006; Wang et al., 1996) but also fine-tuned to ensure precision in lysis timing. In addition to threshold optimization, other aspects of phage λ's holin lysis system seem designed for noise minimization. The phage λ's *S* gene dual start motif, which generates two proteins of opposing function, holin and antiholin, is an archetypal incoherent feedforward circuit. Our previous work showed that, for stable proteins such as holin, feedforward circuits minimize gene expression noise relative to feedback circuits (Ghusinga et al., 2017). In addition, the holin mean burst size (average number of holins produced in a single mRNA lifetime) is estimated to be 1–3 molecules per burst (Chang et al., 1995). Based on our prior FPT moment calculations, such a small protein burst size relative to the event threshold will yield a tight distribution of lysis times (Ghusinga et al., 2017).

Variation in lysis timing, then, may have consequences for phage λ's fitness. This prediction can be tested in future work by comparing the fitness of mutant strains with same mean lysis timing but different noise levels. Positive results from such competition experiments would provide strong evidence that threshold optimization may be an underappreciated constraint on the adaptive evolution of regulatory timing molecules.

With respect to phage life history, our results present an intriguing mystery. What ecological circumstances induce selective pressure favoring noise minimization in phage λ's lysis timing? Previous work suggests that, contrary to our findings, phages should experience selection in favor of increased lysis time variance (Baker et al., 2016; Bull et al., 2011). The reason given for this effect is that early bursts contribute more to fitness than late bursts subtract (Baker et al., 2016; Bull et al., 2011). How can we explain the discrepancy? A recent analysis finds that lysis time will converge on an evolutionarily stable strategy (ESS) that minimizes the amount of resources needed by a phage and maximizes phage fitness (Bonachela and Levin, 2014). The impact on viral fitness of any mutations increasing burst size at the expense of increasing the lysis time is positive until host resources begin to limit the burst size (Bonachela and Levin, 2014). Furthermore, the plot of fitness as a function of the latent period has a narrow hump shape and can be maximized around an optimal value (Bonachela and Levin, 2014). In a stable environment, we might expect that selection favors lysis time genotypes that converge on this optimum, thus minimizing noise (Peng et al., 2016).

Two additional points are germane to this problem. First, the model described above is based on the phage and bacteria interacting in a continuous culture. We note that this type of culture likely better reflects the natural habitat of phage λ, i.e., the mammalian gut, than does serial transfer batch culture. Second, the outcomes described are more likely under consistent environmental conditions, such as those experienced during laboratory propagation. This combination of features may further explain why lysis time noise has been minimized in phage λ. It would be interesting to compare our results with that of other phages isolated more recently, especially those with sophisticated lysis systems.

Limitations of the Study

In this study, we define threshold concentration as a single parameter (α, see Supplemental Information) that combines both membrane insertion rate as well as holin concentration required for triggering membrane lesion formation. A low threshold could mean high rate of membrane insertion (reaching the threshold concentration faster than the wild-type) and/or highly efficient lesion formation due to a functionally improved holin (i.e., fewer molecules are required for triggering thus lowering threshold concentration). In one instance, we clearly demonstrate a lower threshold due to significantly higher rate of membrane accumulation (JJD405, Figure S2) compared with S105. In this case, although it is safe to assume that high rate of membrane insertion is the primary mechanism, one cannot entirely rule out the possibility that the mutant holin is also more efficient in triggering lesion formation. We do not yet clearly understand if these two processes directly affect each other or they can be mutually exclusive. This will be clear once the amino acids that play crucial roles in the different steps leading to lysis has been accurately identified. Therefore, we are currently unable to predict the effects of individual mutations on model parameters. Along the same lines, it is possible that changes in the holin sequence can render it unstable, which is not considered in the current model.

Resource Availability

Lead Contact

Further information and requests for resources should be directed to and will be fulfilled by the Lead Contact, John Dennehy (john.dennehy@qc.cuny.edu).

Materials Availability

All unique/stable reagents generated in this study are available from the Lead Contact without restriction.

Data and Code Availability

Original source data for figures in the paper is available at https://doi.org/10.17632/8t7dxfdgm2.1.

METHODS

All methods can be found in the accompanying Transparent Methods supplemental file.

SUPPLEMENTAL INFORMATION

Supplemental Information can be found online at https://doi.org/10.1016/j.isci.2020.101186.

ACKNOWLEDGMENTS

This work was funded by National Institutes of Health NIGMS grant 1R01GM124446-01 to A.S. and J.J.D. We are grateful for intellectual input from Stephen Abedon, Khem Ghusinga, Fabrizio Spagnolo, Cesar Vargas-Garcia, Daniel Weinreich, and past and present members of the Dennehy Lab. We thank Ryland Young for stimulating conversations about phage λ and for some of the phage and bacterial strains described herein.

AUTHOR CONTRIBUTIONS

Conceptualization, J.J.D. and A.S.; Methodology, S.K., A.S., S.D., and J.J.D.; Investigation, S.K. and T.G.; Formal Analysis, A.S., S.D., and S.K.; Validation, S.K. and T.G.; Visualization, S.K.; Data Curation, S.K.; Resources, I.-N.W. and J.J.D.; Writing – Original Draft, S.K.; Writing – Review & Editing, J.J.D. and A.S.; Project Administration, S.K.; Supervision, J.J.D. and A.S.; Funding Acquisition, A.S. and J.J.D.

DECLARATION OF INTERESTS

The authors declare no competing interests.

Received: April 3, 2020
Revised: May 3, 2020
Accepted: May 15, 2020
Published: June 26, 2020

REFERENCES

Baker, C.W., Miller, C.R., Thaweethai, T., Yuan, J., Baker, M.H., Joyce, P., and Weinreich, D.M. (2016). Genetically determined variation in lysis time variance in the bacteriophage ϕX174. G3 (Bethesda) *6*, 939–955.

Bar-Even, A., Paulsson, J., Maheshri, N., Carmi, M., O'Shea, E., Pilpel, Y., and Barkai, N. (2006). Noise in protein expression scales with natural protein abundance. Nat. Genet. *38*, 636–643.

Bläsi, U., Chang, C.Y., Zagotta, M.T., Nam, K.B., and Young, R. (1990). The lethal lambda S gene encodes its own inhibitor. EMBO J. *9*, 981–989.

Bonachela, J.A., and Levin, S.A. (2014). Evolutionary comparison between viral lysis rate and latent period. J. Theor. Biol. *345*, 32–42.

Bull, J.J., Heineman, R.H., and Wilke, C.O. (2011). The phenotype-fitness map in experimental evolution of phages. PLoS One *6*, e27796.

Cai, L., Friedman, N., and Xie, X.S. (2006). Stochastic protein expression in individual cells at the single molecule level. Nature *440*, 358–362.

Campbell, K.J., and Tait, S.W.G. (2018). Targeting BCL-2 regulated apoptosis in cancer. Open Biol. *8*, 180002.

Chang, C.Y., Nam, K., and Young, R. (1995). S gene expression and the timing of lysis by bacteriophage lambda. J. Bacteriol. *177*, 3283–3294.

Chong, S., Chen, C., Ge, H., and Xie, X.S. (2014). Mechanism of transcriptional bursting in bacteria. Cell *158*, 314–326.

Co, A.D., Lagomarsino, M.C., Caselle, M., and Osella, M. (2017). Stochastic timing in gene expression for simple regulatory strategies. Nucleic Acids Res. *45*, 1069–1078.

Dennehy, J.J., and Wang, I.-N. (2011). Factors influencing lysis time stochasticity in bacteriophage λ. BMC Microbiol. *11*, 174.

Eldar, A., and Elowitz, M.B. (2010). Functional roles for noise in genetic circuits. Nature *467*, 167–173.

Elowitz, M.B., Levine, A.J., Siggia, E.D., and Swain, P.S. (2002). Stochastic gene expression in a single cell. Science *297*, 1183–1186.

Friedman, N., Cai, L., and Xie, X.S. (2006). Linking stochastic dynamics to population distribution:

an analytical framework of gene expression. Phys. Rev. Lett. *97*, 168302.

Ghusinga, K.R., Dennehy, J.J., and Singh, A. (2017). First-passage time approach to controlling noise in the timing of intracellular events. Proc. Natl. Acad. Sci. U S A *114*, 693–698.

Ghusinga, K.R., Vargas-Garcia, C.A., and Singh, A. (2016). A mechanistic stochastic framework for regulating bacterial cell division. Sci. Rep. *6*, 30229.

Gründling, A., Smith, D.L., Bläsi, U., and Young, R. (2000). Dimerization between the holin and holin inhibitor of phage lambda. J. Bacteriol. *182*, 6075–6081.

Gupta, S., Varennes, J., Korswagen, H.C., and Mugler, A. (2018). Temporal precision of regulated gene expression. PLoS Comput. Biol. *14*, e1006201.

Heineman, R.H., Bull, J.J., and Hansen, T. (2007). Testing optimality with experimental evolution: lysis time in a bacteriophage. Evolution *61*, 1695–1709.

Kobiler, O., Rokney, A., Friedman, N., Court, D.L., Stavans, J., and Oppenheim, A.B. (2005). Quantitative kinetic analysis of the bacteriophage lambda genetic network. Proc. Natl. Acad. Sci. U S A *102*, 4470–4475.

Liu, P., Song, R., Elison, G.L., Peng, W., and Acar, M. (2017). Noise reduction as an emergent property of single-cell aging. Nat. Commun. *8*, 680.

Liu, X., Jiang, H., Gu, Z., and Roberts, J.W. (2013). High-resolution view of bacteriophage lambda gene expression by ribosome profiling. Proc. Natl. Acad. Sci. U S A *110*, 11928–11933.

Pang, X., Moussa, S.H., Targy, N.M., Bose, J.L., George, N.M., Gries, C., Lopez, H., Zhang, L., Bayles, K.W., Young, R., and Luo, X. (2011). Active Bax and Bak are functional holins. Genes Dev. *25*, 2278–2290.

Peng, W., Song, R., and Acar, M. (2016). Noise reduction facilitated by dosage compensation in gene networks. Nat. Commun. *7*, 12959.

Raj, A., and van Oudenaarden, A. (2008). Nature, nurture, or chance: stochastic gene expression and its consequences. Cell *135*, 216–226.

Santos, L.C., Vogel, R., Chipuk, J.E., Birtwistle, M.R., Stolovitzky, G., and Meyer, P. (2019). Mitochondrial origins of fractional control in regulated cell death. Nat. Commun. *10*, 1313.

Schneider, B.L., Zhang, J., Markwardt, J., Tokiwa, G., Volpe, T., Honey, S., and Futcher, B. (2004). Growth rate and cell size modulate the synthesis of, and requirement for, G1-phase cyclins at start. Mol. Cell. Biol. *24*, 10802–10813.

Singh, A., and Dennehy, J.J. (2014). Stochastic holin expression can account for lysis time variation in the bacteriophage λ. J. R. Soc. Interface *11*, 20140140.

Song, R., and Acar, M. (2019). Stochastic modeling of aging cells reveals how damage accumulation, repair, and cell-division asymmetry affect clonal senescence and population fitness. BMC Bioinformatics *20*, 391.

Song, R., Peng, W., Liu, P., and Acar, M. (2015). A cell size- and cell cycle-aware stochastic model for predicting time-dynamic gene network activity in individual cells. BMC Syst. Biol. *9*, 91.

Taniguchi, Y., Choi, P.J., Li, G.W., Chen, H., Babu, M., Hearn, J., Emili, A., and Sunney Xie, X. (2010). Quantifying E. coli proteome and transcriptome with single-molecule sensitivity in single cells. Science *329*, 533–538.

Wang, I.-N. (2006). Lysis timing and bacteriophage fitness. Genetics *172*, 17–26.

Wang, I.N., Dykhuizen, D.E., and Slobodkin, L.B. (1996). The evolution of phage lysis timing. Evol. Ecol. *10*, 545–558.

Wang, I.-N., Smith, D.L., and Young, R. (2000). Holins: the protein clocks of bacteriophage infections. Annu. Rev. Microbiol. *54*, 799–825.

White, R., Chiba, S., Pang, T., Dewey, J.S., Savva, C.G., Holzenburg, A., Pogliano, K., and Young, R. (2011). Holin triggering in real time. Proc. Natl. Acad. Sci. U S A *108*, 798–803.

White, R., Tran, T.A.T., Dankenbring, C.A., Deaton, J., and Young, R. (2010). The N-terminal transmembrane domain of lambda S is required for holin but not antiholin function. J. Bacteriol. *192*, 725–733.

Young, R. (2014). Phage lysis: three steps, three choices, one outcome. J. Microbiol. *52*, 243–258.

Yurkovsky, E., and Nachman, I. (2013). Event timing at the single-cell level. Brief. Funct. Genomics *12*, 90–98.

iScience, Volume *23*

Supplemental Information

Optimum Threshold Minimizes Noise in Timing of Intracellular Events

Sherin Kannoly, Tianhui Gao, Supravat Dey, Ing-Nang Wang, Abhyudai Singh, and John J. Dennehy

Supplementary Information

Transparent Methods

Bacterial and phage strains

All the bacteria and plasmids used in this study are listed in Table S1. *E. coli* lysogens were cultured in lysogeny broth (LB) at 30°C with rotary shaking (220 rpm).

Table S1. List of bacterial strains and plasmids used in this study. Lambda lysogens constructed with these strains are listed in Table 1 of the main text.

Strain	Genotype	Source
CGSC#: 6152[a]	*E. coli* MC4100 (λ-)	(Casadaban, 1976)
S::Cam	MC4100 (λ cI857 *S*::*Cam*)	(Shao and Wang, 2008)
JJD3	MC4100 (λ cI857 *S*)	(Wang, 2006)
JJD5	MC4100 (λ cI857 *S105*)	(Wang, 2006)
pUCS105R-	pUC18 (λ lysis cassette)	(Shao and Wang, 2008)

[a]Coli Genetic Stock Center

Construction of plasmids with mutations in holin

Briefly, site-directed mutagenesis was used to generate a panel of mutant λ phages with one or two base pair substitutions in the *S105* allele of the holin gene. Plasmid pUCS105R- carries the λ lysis cassette with the *S105* allele, which has a Leu (CUG) codon in place of the Met1 codon of the *S* gene. This plasmid was used as a template for PCR (Pfu DNA polymerase; Promega, Madison, WI) using megaprimers consisting of 30 to 45-nucleotide homology flanking the altered nucleotides. After *DpnI* treatment to digest the original template, the resulting plasmids were transformed into MC4100 (λ cI857 *S*::*Cam*) cells. The cells were spread on LB + Amp (100 μg ml^{-1}) plates and incubated at 30°C until colonies were visible. Some of the plasmids thus constructed were further used as templates to generate double mutants.

Transferring mutant holin from the plasmid into the λ phage genome

Transformed MC4100 (λ cI857 *S*::*Cam*) cells were grown in 3 ml LB supplemented with ampicillin (100 μg ml^{-1}) at 30°C in a rotary shaker. For thermal induction of prophages, the cultures were transferred to a shaker at 42°C for 15 min and then 37°C until lysis. The resulting lysate was plated with MC4100 cells to obtain plaque-forming phages resulting from recombination between the prophage and the plasmid. To obtain lysogens, phages obtained from the plaques were used to infect 100 μl of saturated MC4100 culture for 30 min. To this culture, 1 ml LB broth was added and further incubated at 30°C in a rotary shaker for 1 h. A 100 μl aliquot of this mixture was spread on LB plates supplemented with kanamycin (50 μg ml^{-1}), and incubated overnight at 30°C. The lysogens were further screened for ampicillin resistance followed by DNA sequencing to confirm the nucleotide substitutions.

Single-cell lysis time determination

The protocol for determining single-cell lysis times has been described previously (Dennehy and Wang, 2011). Briefly, lysogens were grown overnight in LB at the permissive temperature of 30°C. Overnight cultures were diluted 100-fold and grown to A_{550} = 0.3–0.4 in a 30 °C shaking incubator. A 200-μl aliquot of the exponentially growing culture was immobilized to a 22 mm square glass coverslip, which was pretreated with 0.01% poly-L-lysine (mol. wt. 150 K–300 K; Millipore Sigma, St. Louis, MO) at room temperature for 10 min, and applied to a perfusion chamber (RC-21B, Warner Instruments, New Haven, CT). After assembly, the perfusion chamber was immediately placed on a heated platform (PM2; Warner Instruments, New Haven, CT), which was mounted on an inverted microscope stage (TS100, Nikon, Melville, NY), and infused with heated LB at 30°C (Inline heater: SH-27B, dual channel heating controller: TC-344B; Warner Instruments, New Haven, CT). The chamber temperature was spiked to 42°C for 20 min, then maintained at 37°C until ~95% lysis was observed. Videos were recorded using an eyepiece camera (10X MiniVID™; LW Scientific, Norcross, GA, 10 fps), and the lysis times of individual cells were visually ascertained using VLC™ media player. Lysis time was defined as the time required for a cell to disappear after the temperature was increased to 42 °C.

S1. Lysis time determination of batch cultures using a plate reader

After sequence confirmation, the lysogens were first heat-induced in batch cultures to assess their lysis times. A 5-µL aliquot of overnight cultures was mixed with 1 mL LB in 24-well plates. Following growth at 30°C for 2 h, the plates were shifted to a 42°C water bath (time 0 for lysis time) for 15 min. After heat induction, the plates were shifted to a pre-warmed plate reader (Synergy™ HT, BioTek® Instruments, Inc., Vermont, USA) at 37°C, which measures A_{550} of the culture every 2 min. This protocol was repeated in triplicate for all 350 lysogens. The complementary cumulative distribution function of the normal distribution was used to fit the A_{550} outputs generated by the plate reader. The estimated mean and standard deviation were defined as the lysis time and spread respectively. FPTs estimated using both the batch culture and single-cell recordings are strongly correlated (Figure S1).

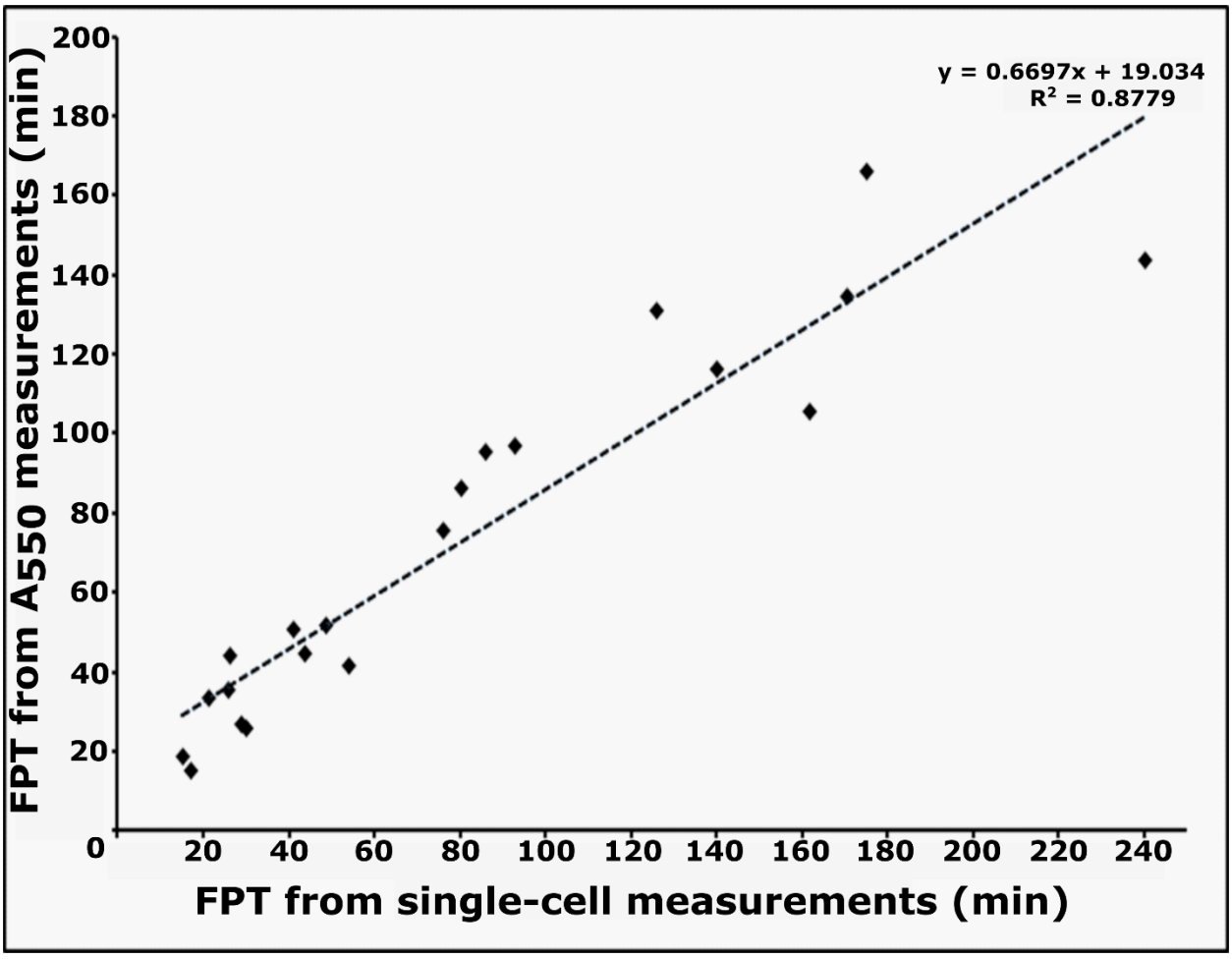

Figure S1. The FPT measurements using A_{550} and single-cell recordings are strongly correlated. This figure references the strains identified in Table 1 in the main text.

S2. Holin expression

We extracted holin from whole cells as well as cell membranes to compare the relative holin levels in different mutant strains. An exponentially growing culture (A_{600} ~0.4) at 30°C was induced at

42°C for 20 min. A 5 mL aliquot of the culture was centrifuged to pellet the cells. The pellets were mixed with 2× SDS-PAGE sample buffer, heated at 100°C for 5 min, and loaded on a 4-20% TruPAGE^{TM} precast gel (SIGMA-ALDRICH, St. Louis, MO, USA). Another 4 ml aliquot of the culture was sonicated to disrupt the membranes. The membranes were collected by centrifugation at 100,000 × g for 1 h. The pelleted membranes were mixed with 40 µl of ME buffer (10 mM Tris Cl [pH 8.0], 35 mM $MgCl_2$, 1% Triton X-100) by shaking on a platform shaker for 2 h at 25°C. The extracted samples were centrifuged at 100,000 × g for 30 min to pellet the insoluble fraction. The membrane extracts were mixed with 2× SDS-PAGE sample buffer, heated at 100°C for 3 min, and loaded on to precast gels. After electrophoresis, Western blotting was used to detect holin using a primary antibody (1:1000) raised in rabbits. A secondary antibody (donkey anti-rabbit polyclonal antibody conjugated to horseradish peroxidase [SA1-200, Pierce Chemicals]) was used at a dilution of 1:1000 dilution, and the blot was developed as per the manufacturer's directions. An average of three preparations was used to estimate holin levels.

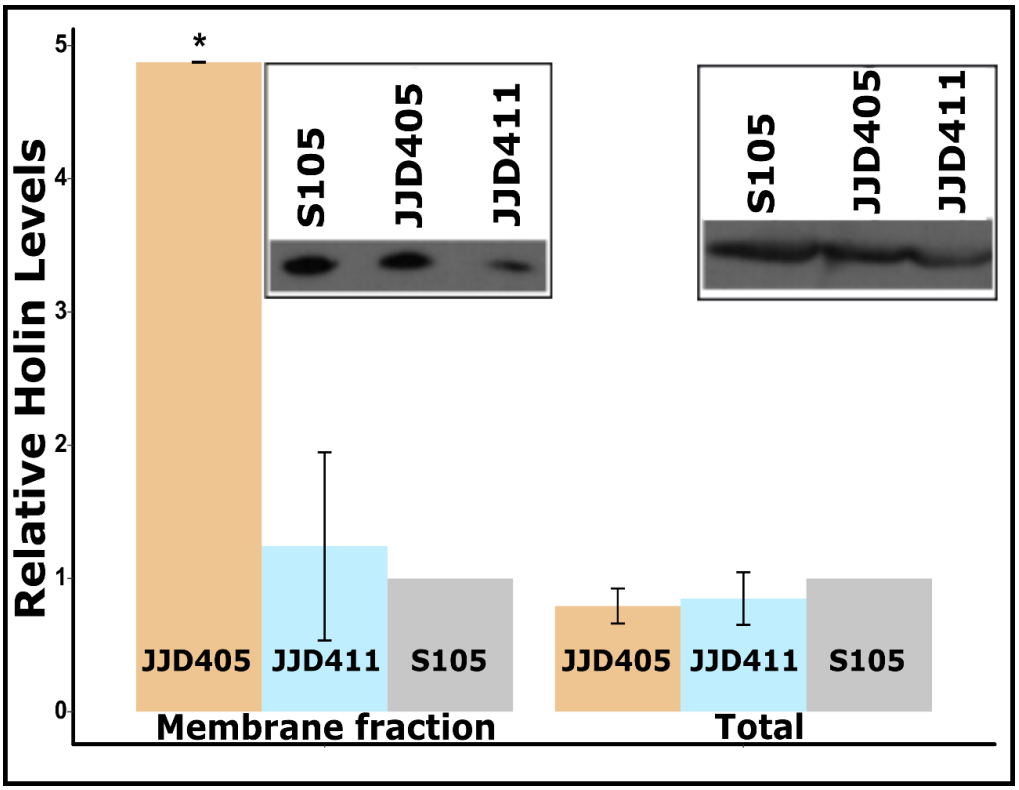

Figure S2. Total holin levels from whole-cell extracts and membrane fractions. The left and right panels show western blots of membrane fractions and whole-cell extracts, respectively. Bands represent holin extracted from strains S105 (mean LT = 58 min), JJD405 (32 min), and JJD411 (176 min). *, $p < 0.05$, t-test; error bars, mean ± SEM. Strains shown here reference Table 1 in the main text.

Calculation of noise in the first passage time

We model the expression of holin occurring in intermittent bursts, with burst events arriving as a Poisson process with rate *k*. Whenever a burst occurs, the total cellular concentration of holin $x(t)$ at time *t* increases by a random amount b:

$$x(t) \mapsto x(t) + b, \tag{S1}$$

where b is drawn from an arbitrary positively-valued probability distribution with the first and second moments $\langle b \rangle$ and $\langle b^2 \rangle$, respectively. The first moment $\langle b \rangle$ represents the mean burst size per unit volume. Between two consecutive bursts, the concentration diluters from cell growth as per the following the deterministic dynamics:

$$\dot{x}(t) = -\gamma x(t) \tag{S2}$$

where γ is the cellular growth rate. For this hybrid system with stochastic bursts interspersed by first-order decay, the time evolution of the first and second-order moments of $x(t)$ are given by

$$\frac{d\langle x \rangle}{dt} = k\langle b \rangle - \gamma\langle x \rangle, \tag{S3}$$

$$\frac{d\langle x^2 \rangle}{dt} = k\langle b^2 \rangle + 2k\langle b \rangle\langle x \rangle - 2\gamma\langle x^2 \rangle, \tag{S4}$$

(Friedman et al., 2006; Hespanha and Singh, 2005; Singh and Hespanha, 2011). Solving the above differential equations, we get the mean $\langle x \rangle$ and variance $\langle x^2 \rangle - \langle x \rangle^2$ of the holin concentration as a function of time t, assuming there is no holin at the onset of the protein synthesis;

$$\langle x \rangle = \frac{[1 - e^{-\gamma t}]\, k\, \langle b \rangle}{\gamma} \tag{S5}$$

$$\langle x^2 \rangle - \langle x \rangle^2 = \frac{[1 - e^{-2\gamma t}]\, k\, \langle b^2 \rangle}{2\,\gamma}. \tag{S6}$$

We formulate the lysis time as the first-passage time

$$FPT = \min\{t : x(t) \geq X | x(0) = 0\}, \tag{S7}$$

or the first time the holin concentration reaches a critical threshold level X, and quantify the noise in the first-passage time using the coefficient of variation squared,

$$CV_{FPT}^2 = (\langle FPT^2 \rangle - \langle FPT \rangle^2)/\langle FPT \rangle^2, \tag{S8}$$

where $\langle FPT \rangle$ and $\langle FPT^2 \rangle$ are the first two moments of *FPT*. CV_{FPT}^2 is related to the fluctuations in the holin concentration as per

$$CV_{FPT}^2 \approx \frac{\langle x^2 \rangle - \langle x \rangle^2}{\langle FPT \rangle^2} \left(\frac{d\langle x \rangle}{dt} \right)^{-2} \Bigg|_{t = \langle FPT \rangle}, \tag{S9}$$

(Co et al., 2017). From eq. S5 the mean first-passage time is obtained as

$$\langle FPT\rangle = -\frac{1}{\gamma}\log(1-\alpha), \text{ with } \alpha = \frac{X}{x_s}. \quad S10$$

Here x_s denotes the steady-state mean holin concentration and is given by,

$$x_s = \langle x(t\to\infty)\rangle = \frac{k\langle b\rangle}{\gamma}, \quad S11$$

with the underlying assumption in eq. S10 being that the threshold for lysis *X* is less than x_s. Using equations (S5), (S6), and (S9), we write down the formula for the noise in *FPT*,

$$CV^2_{FPT} = CV^2_x \frac{\alpha\,(2-\alpha)}{[(1-\alpha)\ln(1-\alpha)]^2}, \quad S12$$

where, CV^2_x is the coefficient of variation squared for the holin concentration at steady state

$$CV^2_x = \lim_{t\to\infty}\frac{\langle x^2\rangle - \langle x\rangle^2}{\langle x\rangle^2} = \frac{\langle b^2\rangle}{2\langle b\rangle x_s} \quad S13$$

and quantifies the extent of stochasticity in holin expression. The above formula can be rewritten in terms of $\langle FPT\rangle$ as,

$$CV^2_{FPT} = CV^2_x \frac{\left[e^{2\gamma\langle FPT\rangle}-1\right]}{(\gamma\langle FPT\rangle)^2} \quad S14$$

and varies nonmonotonically with the mean FPT consistent with experimental data. The optimal value of the mean FPT (in the unit of γ^{-1}), where noise is minimum is $\gamma\langle FPT\rangle \approx 0.8$. The corresponding value of the threshold (in the unit of steady state concentration) is $\alpha = \frac{X}{x_s} \approx 0.55$.

References

Casadaban, M.J. (1976). Transposition and fusion of the lac genes to selected promoters in Escherichia coli using bacteriophage lambda and Mu. J. Mol. Biol. 104, 541–555.

Co, A.D., Lagomarsino, M.C., Caselle, M., Osella, M. (2017). Stochastic timing in gene expression for simple regulatory strategies. Nucleic Acids Res. 45, 1069–1078.

Dennehy, J.J., Wang, I.-N. (2011). Factors influencing lysis time stochasticity in bacteriophage λ. BMC Microbiol. 11, 174.

Friedman, N., Cai, L., Xie, X.S. (2006). Linking stochastic dynamics to population distribution: An analytical framework of gene expression. Phys. Rev. Lett. 97, 168302

Hespanha, J.P., Singh, A. (2005). Stochastic models for chemically reacting systems using polynomial stochastic hybrid systems. Int. J. Robust Nonlinear Control 15, 669–689.

Shao, Y., Wang, I.-N. (2008). Bacteriophage adsorption rate and optimal lysis time. Genetics 180, 471–482.

Singh, A., Hespanha, J.P. (2011). Approximate moment dynamics for chemically reacting systems. IEEE Trans. Autom. Control 56, 414–418.

Wang, I.-N. (2006). Lysis timing and bacteriophage fitness. Genetics 172, 17–26.